

A CVD Process for Producing Atomic Current Sources Based on ^{63}Ni

I. D. Kharitonov^a, V. A. Mazgunova^b, V. A. Babain^b, A. I. Kostylev^b,
A. O. Merkushev^c, A. A. Shemukhin^d, Yu. V. Balakshin^d, A. V. Kozhemyako^d,
S. N. Kalmykov^a, and E. P. Magomedbekov^{*c}

^a Chemical Faculty, Moscow State University, Moscow, Russia

^b Khlopin Radium Institute, 2-i Murinskii pr. 28, St. Petersburg, 194021 Russia

^c Mendeleev University of Chemical Technology of Russia, Miusskaya pl. 9, Moscow, 125047 Russia

^d Skobeltsyn Institute of Nuclear Physics, Moscow State University, Moscow, Russia

*e-mail: eldar@rctu.ru

Received May 10, 2017

Abstract—A CVD process was developed for producing ^{63}Ni -based atomic batteries by deposition of active ^{63}Ni layers onto semiconductor silicon supports. Tetrakis(trifluorophosphine)nickel synthesized from ^{63}Ni metal and phosphorus trifluoride was used as the volatile precursor. The influence of the support temperature and working pressure on the characteristics of the ^{63}Ni coating was examined.

Keywords: atomic batteries, nickel-63, chemical vapor deposition, tetrakis(trifluorophosphine)nickel

DOI: 10.1134/S1066362218020054

Atomic batteries (ABs) containing radioactive isotopes such as ^{90}Sr , ^{238}Pu , ^{227}Ac , etc., show promise for the development of a new generation of autonomous microwatt power sources characterized by long operation life (>20 years), high specific power, small size, safety, and operation stability in a wide temperature range [1].

Atomic batteries operating on the basis of the β -voltaic effect with ^{63}Ni as a working radioactive isotope meet the safety and efficiency requirements to the greatest extent [2, 3]. A β -voltaic converter (Fig. 1a) is a semiconductor cell with p - n transition, contacting with a radioactive source of β -particles (i.e., electrons). Pairs of charge carriers are generated via transfer of the energy of β -particles upon their interaction with electrons of the crystal lattice, and the amount of the generated nonequilibrium carriers is proportional to the incident particle flux energy.

The advantages of ^{63}Ni compared to the majority of other β -emitting nuclides are long half-life (100 years) and low β -particle energy ($E_{\text{av}} = 17$ keV). The external shell of the device absorbs the β -radiation of such energy completely [4, 5].

The performance of a β -voltaic battery is determined by characteristics of both the semiconductor converter (efficiency of the conversion of the β -particle energy to electricity) and the ^{63}Ni layer. It is necessary to obtain a homogeneous, uniform, and

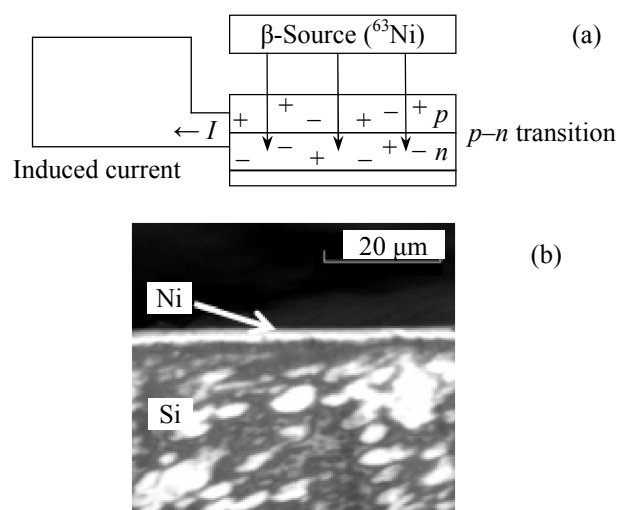


Fig. 1. Operation principle of a β -voltaic current source: (a) schematic presentation and (b) electron microscopic image of a Ni layer.

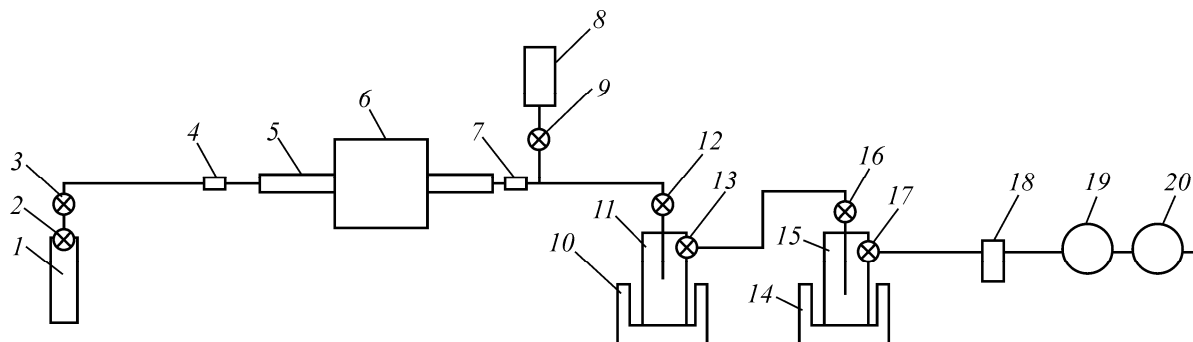


Fig. 2. Scheme of the installation for deposition of thin ^{63}Ni films onto semiconductor supports: (1) cylinder with $\text{Ni}(\text{PF}_3)_4$, (2, 9, 12, 13, 16, 17) locking valves, (3) fine control valve, (4, 7) connecting tubes, (5) reaction vessel, (6) rotary tubular furnace, (8) pressure gage, (10, 14) Dewar vessels, (11) condenser for $\text{Ni}(\text{PF}_3)_4$, (15) condenser for fluorinated waste, (18) nitrogen trap, (19) turbo-molecular pump, and (20) mechanical pump.

dense conducting coating approximately $2\ \mu\text{m}$ thick (to exclude the self-absorption loss) from nickel with no less than 70–80% ^{63}Ni enrichment. This coating should also exhibit high adhesion to the semiconductor support.

Various methods are known for depositing nickel coatings. These include, e.g., the electrochemical method [10] or CVD method using nickel tetracarbonyl [6–9] or organometallic nickel compounds [11–13]. Electrochemical deposition involves problems with adhesion, nonuniform coating, and loss of the initial expensive isotope. The use of nickel carbonyl in the process is impossible because of its low thermal stability and fire and explosion hazard, which is critical when working with a radioactive material. Synthesis of more complex nickel organometallic compounds involves loss of the material, complicated regeneration procedure, and large amount of radioactive waste.

In this study, we chose tetrakis(trifluorophosphine)-nickel $\text{Ni}(\text{PF}_3)_4$ as the starting nickel compound for the deposition of nickel layers. It can be synthesized in a high yield from nickel metal and phosphorus trifluoride [14]. $\text{Ni}(\text{PF}_3)_4$ under normal conditions is a transparent liquid with the freezing point of -55°C and boiling point of 70.5°C . Tetrakis(trifluorophosphine) nickel is thermally stable up to 150°C , in contrast to nickel carbonyl decomposing at temperatures of the order of $60\text{--}70^\circ\text{C}$. $\text{Ni}(\text{PF}_3)_4$ is relatively stable in air, incombustible, and explosion-safe, which is favorable for the technology. Another important factor is that all the constituent atoms of the compound (except Ni) consist of single isotopes. Therefore, $\text{Ni}(\text{PF}_3)_4$ is suitable for use in isotope enrichment processes in the production of ^{63}Ni .

EXPERIMENTAL

An installation schematically shown in Fig. 2 was developed for experiments on deposition of nickel coatings.

In the first step, we performed experiments with $\text{Ni}(\text{PF}_3)_4$ containing nickel of natural isotope composition. As semiconductor supports we used $20 \times 20\ \text{mm}$ silicon plates $200\ \mu$ thick, equipped with silver current collector. The external appearance of the support is shown in Fig. 3.

Experiments were performed at support temperatures in the range $100\text{--}500^\circ\text{C}$ and constant residual pressure of 6–7 Pa. The time of the nickel coating deposition was 2 min.

The installation (Fig. 2) operates as follows. A cylinder with $\text{Ni}(\text{PF}_3)_4$ (1) is connected to reaction vessel 5 via connecting tube 4. A semiconductor support is placed into reaction vessel 5. The system con-

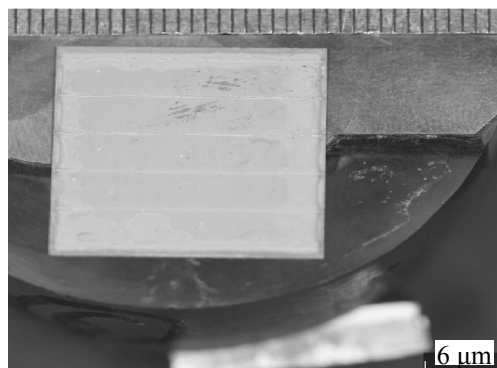


Fig. 3. External appearance of the semiconductor silicon support used in the experiments.

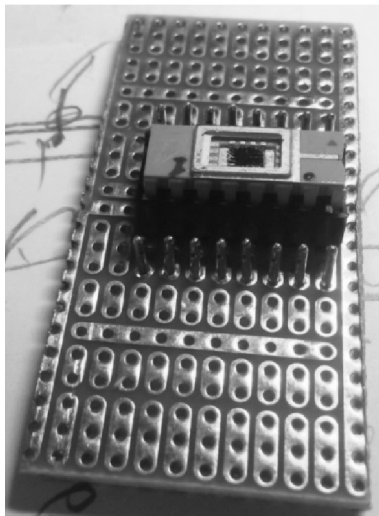


Fig. 4. Photograph of the stage for conductivity measurements.

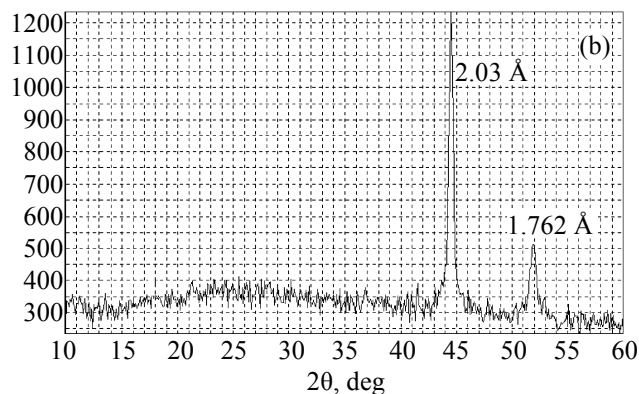
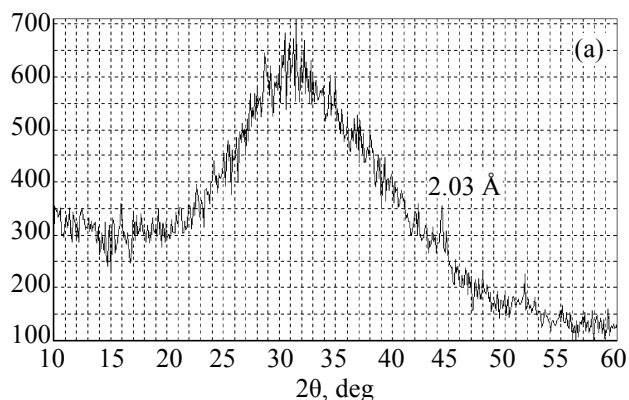


Fig. 5. Diffraction patterns of samples with Ni coatings deposited at different support temperatures: (a) 200 and (b) 400°C.

taining pipelines, reaction vessel 5, and condensers 11 and 15 is evacuated using vacuum system 18–20 to a residual pressure no higher than 10^{-1} Pa. On reaching this pressure, heating of reaction vessel 5 in rotary fur-

nace 6 is switched on. At the fine control valve 3 closed, the locking valve 2 on the cylinder with $\text{Ni}(\text{PF}_3)_4$ is opened. Then, the fine control valve 3 is slowly opened for feeding the gas to reaction vessel 5. The working pressure of 6–7 Pa is set. The pressure is monitored with pressure gage 8.

At temperatures higher than 155°C, $\text{Ni}(\text{PF}_3)_4$ decomposes into nickel metal and phosphorus trifluoride. Nickel metal in the form of a thin film is deposited onto a support (a small amount of the metal in the form of powder and thin flakes is deposited on the reaction vessel walls), and phosphorus trifluoride is removed from the reaction zone using the vacuum system.

Condenser 11 is cooled to -75°C , and condenser 15, to -193°C . Phosphorus trifluoride is collected in condenser 15, and the unchanged $\text{Ni}(\text{PF}_3)_4$ is collected in condenser 11 to exclude its loss and is recycled.

The samples obtained were examined by scanning electron microscopy (SEM) and X-ray diffraction (XRD). Also, the sample conductivity was determined using a specially developed stage (Fig. 4).

RESULTS AND DISCUSSION

At support temperatures lower than 200°C, the efficiency of the $\text{Ni}(\text{PF}_3)_4$ utilization was less than 2%, and the major fraction of $\text{Ni}(\text{PF}_3)_4$ (>98%) remained unchanged and passed into the trap (condenser 11, Fig. 2). At temperatures higher than 450°C, $\text{Ni}(\text{PF}_3)_4$ underwent intense homogeneous decomposition in the gas phase with the formation of a finely dispersed nickel powder depositing in the form of a loose, weakly bound layer on the surface of the reaction vessel.

The surface color of the coatings obtained at different temperatures varies from mirror silvery (at 200°C) to dark gray (at 400°C). The coating sample obtained at 200°C (Fig. 5a) is X-ray amorphous with low content of crystalline Ni. The diffraction patterns of the samples obtained at a support temperature of 400°C demonstrate the presence of the crystalline nickel phase (cubic system, Fig. 5b).

The SEM images of the coating surface (Fig. 6) show that the nickel coating is uniformly distributed over the support. However, the shape of conglomerates forming the layer is different depending on the process conditions. With increasing temperature, the structure consisting of coarse amorphous conglomerates gives way to a dense crystalline structure, which is proved

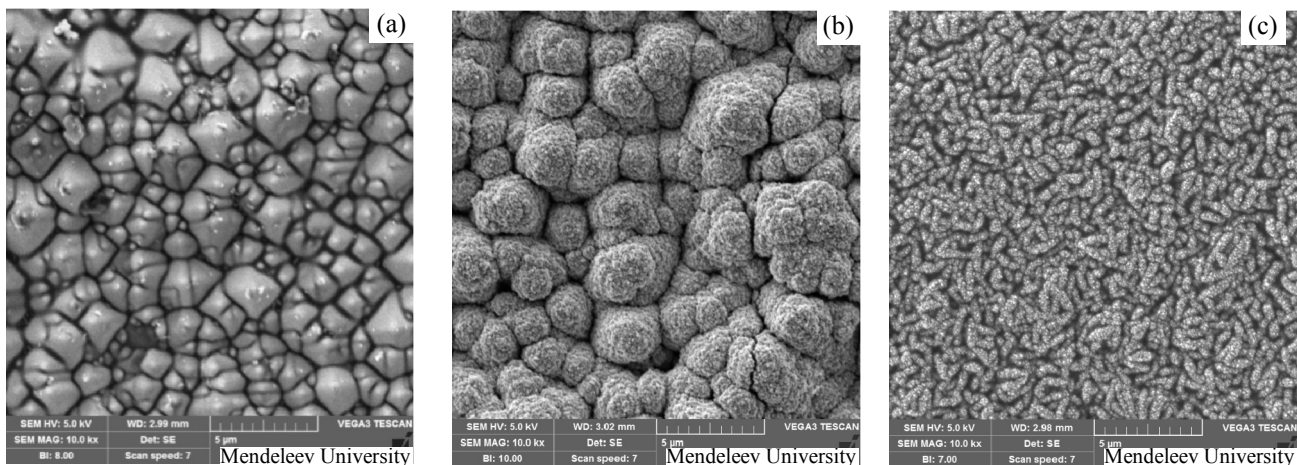


Fig. 6. Electron micrographs of the surfaces of the samples prepared by CVD at different temperatures: (a) 200, (b) 350, and (c) 400°C.

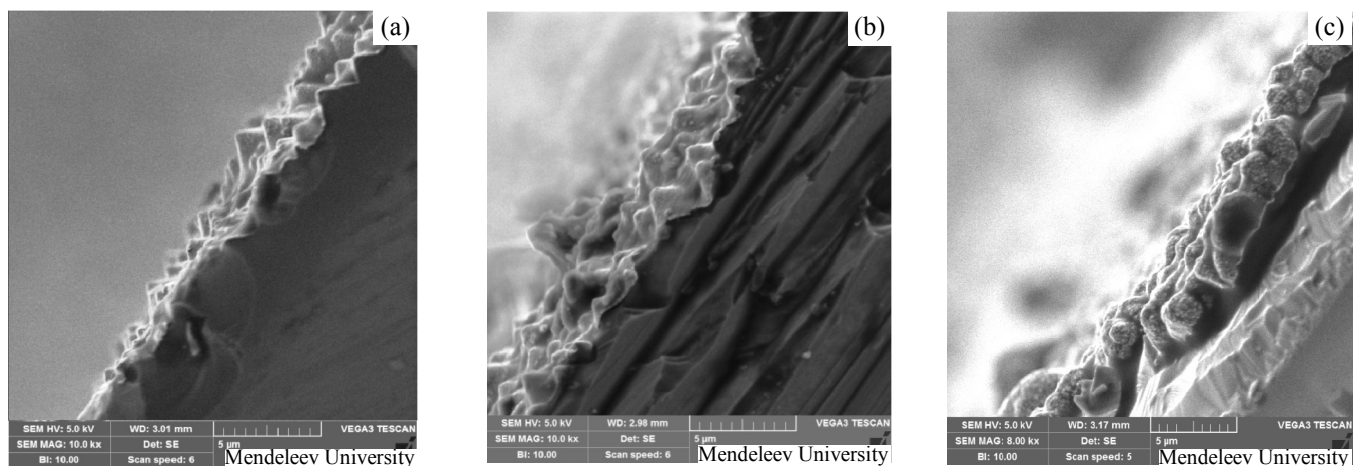


Fig. 7. Images of the break surface of samples obtained at different temperatures: (a) 200, (b) 350, and (c) 400°C.

by the X-ray diffraction pattern. Simultaneously, the coating becomes denser (visually) and more uniform (Fig. 7), and its specific electrical resistivity decreases (Fig. 8).

The Rutherford backscattering (RBS) spectra of the samples were obtained at an HVEE 500 cascade ion accelerator at the Skobeltsyn Institute of Nuclear Physics, Moscow State University [15, 16]. These spectra allowed estimation of the thickness and composition of the surface layer of the power source. The spectra were taken using an analyzing beam of 860-keV He^{2+} ions. The detectable scattering angle was 160° . The RBS spectra were recorded between silver contacts.

As seen from the RBS spectrum shown in Fig. 9, the initial structure consists of a Si *p*-layer (300th channel) and a protective silicon nitride layer (550th

channel) with the inclusion of silver (plateau up to 860th channel), most probably originating from the contacts. After the Ni deposition by the CVD process, followed by annealing at 200°C, the deposited layer

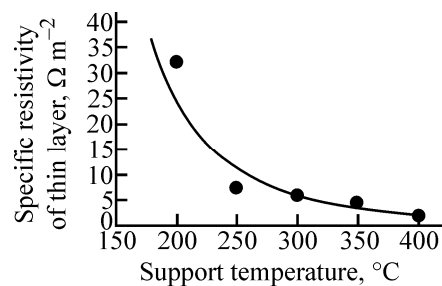


Fig. 8. Specific conductivity per unit area of the nickel layer as a function of the semiconductor support temperature.

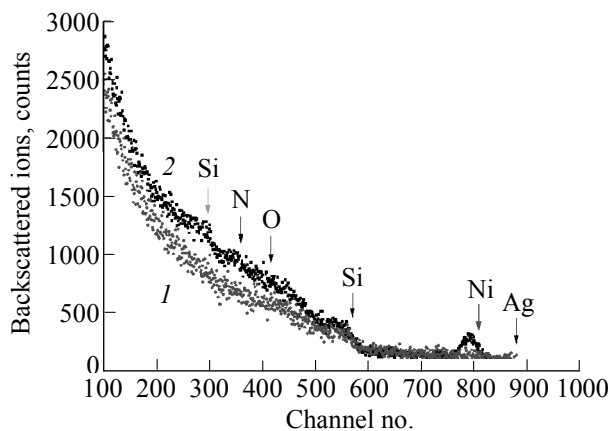


Fig. 9. Energy spectrum of backscattered He^{2+} ions with an energy of 860 keV for a scattering angle of 160° . (1) Initial structure and (2) after Ni deposition and high-temperature treatment at 200°C .

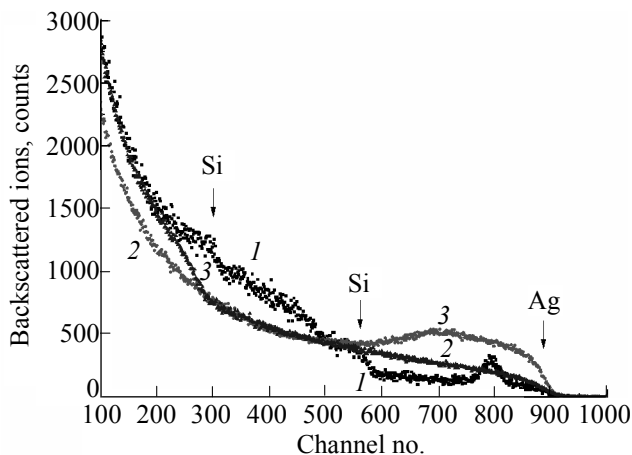


Fig. 10. Energy spectrum of backscattered He^{2+} ions with an energy of 860 keV for a scattering angle of 160° after the Ni deposition and high-temperature treatment at (1) 200, (2) 350, and (3) 400°C .

thickness was 34 ± 8 nm. This scatter can be attributed to the fact that the support surface has developed topography (Figs. 6 and 7). This fact strongly complicates the interpretation of the RBS spectra, because the scattering angle for the backscattered particles varies in a wide range. Annealing resulted in an increase in the nitrogen concentration (350th channel) and in the appearance of oxygen (400th channel) in the surface layers.

As the treatment temperature (Fig. 10) is increased to 350°C , the signal from the backscattered ions (600–900th channels) sharply increases. This is due to the

onset of fusion of the silver contacts. Simultaneously, the signal from oxygen and nitrogen in the 300–500th channels decreases, suggesting a considerable decrease in the concentration of these ions in the surface layers. As the temperature is increased further to 400°C , a continuous weakly sloping front from the 300th to the 900th channel appears. This fact indicates that the elements in the surface layer have underwent uniform mixing, so that it becomes impossible to reveal by RBS the boundary between the nickel layer, protective silicon nitride layer, and silicon *p*-layer.

Thus, we have examined the possibility of depositing nickel coatings from tetrakis(trifluorophosphine)-nickel $\text{Ni}(\text{PF}_3)_4$ by the CVD method on the surface of silicon semiconductor structures. A dense uniform crystalline nickel layer with high electrical conductivity is formed at a support temperature of 400°C , working pressure of 6–7 Pa, and coating growth rate of 0.1 – $0.2 \mu\text{m min}^{-1}$. The data obtained prove good prospects for using the CVD process with tetrakis(trifluorophosphine)nickel as a precursor for fabrication of atomic β -voltaic batteries based on ^{63}Ni .

ACKNOWLEDGMENTS

The study was performed within the framework of Subsidy Agreement no. 14.577.21.0008 of June 5, 2014 (project identification number RFMEFI57714X0008) and was financially supported by the Ministry of Education and Science of the Russian Federation.

REFERENCES

1. Baranov, V.Yu., Pal', A.F., Pustovalov, A.A., et al., Radioisotope generators of electric current, *Izotopy II. Svoystva. Poluchenie. Primenenie* (Isotopes II. Properties. Production. Use), Baranov, V.Yu., Ed., Moscow: Fizmatlit, 2005.
2. Kavetskii, A.G., Nekhoroshkov, S.N., Meleshkov, S.P., and Ustinov, V.A., *Effektivnost' preobrazovaniya energii v betavol'taicheskikh batareyakh* (Efficiency of Energy Conversion in Betavoltaic Batteries), St. Petersburg: Radiyevyi Inst. im. V.G. Khlopina, 2001.
3. Lavrus, V.S., *Batareiki i akkumulyatory* (Cells and Batteries), 1995, <http://www.n-t.org/ii/ba>.
4. Gusev, N.G., Mashkovich, V.P., and Suvorov, A.P., *Fizicheskie osnovy zashchity ot izlucheniya* (Physical Principles of Radiation Protection), Moscow: Atomizdat, 1980.
5. *Tablitsy fizicheskikh velichin: Spravochnik* (Tables of Physical Quantities: Handbook), Moscow: Atomizdat, 1976.

6. *Chem. Eng.*, 1949, vol. 56, no. 10, p. 118/
7. Peterson, D., Non-vacuum deposition techniques for use in fabricating thin film circuits, *Final Report*, 1967, no. 91 336.
8. Syrkin, V.G. and Kir'yanov, Yu.G., *Zh. Prikl. Khim.*, 1970, vol. 43, no. 5, pp. 1068–1073.
9. Skibo, M. and Greulich, F.A., *Thin Solid Films*, 1984, vol. 113, p. 225.
10. Vansovskaya, K.M., *Gal'vanicheskie pokrytiya* (Electroplated Coatings), Leningrad: Mashinostroenie, 1984.
11. Van Hemert, R.L., Spendlove, L.B., and Sievers, R.E., *J. Electrochem. Soc.*, 1965, vol. 112, p. 1123.
12. Van den Brekel, C.H.J., Fonville, R.M.M., van der Straten, P.J.M., and Verspui, G., *Proc. 8th Int. Conf. on Chemical Vapor Deposition*, Blocher, J.M., Jr., Vuillard, G.E., and Wahl, G., Eds., Pennington, NJ: Electrochemical Soc., 1981, p. 142.
13. Park, J.-H. and Sudarshan, T.S., *Chemical Vapor Deposition*, ASM Int., 2001.
14. Kruck, Th., *Angew. Chem. Int. Ed.*, 1967, vol. 6, p. 53.
15. Shemukhin, A.A., Chernykh, P.N., Chernysh, V.S., et al., *Prikl. Fiz.*, 2013, no. 5, pp. 59–62.
16. Shemukhin, A.A., Nazarov, A.V., Balakshin, Yu.V., and Chernysh, V.S., *Nucl. Instrum. Meth. Phys. Res. B*, 2015, vol. 354, p. 274.

Translated by G. Sidorenko